

# Two Higgs Doublet Model from Six Dimensional Gauge Theory

Kento Akamatsu<sup>a</sup>, Takuya Hirose<sup>b</sup>, Nobuhito Maru<sup>a,c</sup> and Akio Nago<sup>a</sup>

<sup>a</sup>*Department of Physics, Osaka Metropolitan University,  
Osaka 558-8585, Japan*

<sup>b</sup>*Faculty of Science and Engineering, Kyushu Sangyo University,  
Fukuoka 813-8503, Japan*

<sup>c</sup>*Nambu Yoichiro Institute of Theoretical and Experimental Physics (NITEP),  
Osaka Metropolitan University, Osaka 558-8585, Japan*

## Abstract

We improve our previously proposed two Higgs doublet model of six-dimensional  $SU(4)$  gauge theory compactified on an orbifold  $T^2/Z_2$  by introducing the brane localized gauge kinetic terms. Since two Higgs doublets are identified with massless zero modes in extra spatial components of the six-dimensional gauge field, the Higgs sector in our model is constrained by the six-dimensional gauge symmetry. As a result, our Higgs potential at tree-level is automatically CP conserving and  $Z_2$  symmetric, which are assumed by hand in the ordinary two Higgs doublet models. The scalar masses breaking the  $Z_2$  symmetry softly are generated at one-loop. We show that the Standard Model Higgs mass can be obtained by tuning the size of the brane localized gauge kinetic terms as well as the electroweak symmetry breaking is realized. Other physical Higgs masses are predicted.

# 1 Introduction

Two Higgs Doublet Model (2HDM) is one of the interesting extensions of the Standard Model (SM), where an additional Higgs doublet is introduced to the SM and its experimental aspects are extensively studied [1–3]. Since the 2HDM has five physical Higgs scalars, its phenomenology is much richer than the that of the SM. Although the 2HDM is very attractive, some assumptions in tree-level potential are usually imposed by hand for phenomenological problems. First, a softly broken  $Z_2$  symmetry is assumed to avoid Flavor Changing Neutral Current (FCNC) processes at tree-level. Second, CP symmetry is assumed. Furthermore, the gauge hierarchy problem is not solved and the Higgs mass cannot be predicted in the 2HDM.

Starting from higher-dimensional gauge theories as the Beyond SM, the massless zero modes in extra components of the higher-dimensional gauge fields can be regarded as the Higgs fields, which is an idea of gauge-Higgs unification (GHU) [4–11]. In particular, two Higgs doublets originate from the massless zero modes of  $A_{5,6}$  in the six-dimensional (6D) gauge field, where the Higgs sector is therefore controlled by the 6D gauge symmetry in a sense of GHU [12–18]. In these 6D models, the tree-level masses of two Higgs doublets are forbidden by the 6D gauge symmetry and the mass spectra in the Higgs sector are predicted by taking the one-loop quantum corrections into account. In particular, the SM Higgs mass squared is finite at one-loop, which is roughly an order of a square root of one-loop factor times a compactification scale. Since the compactification scale is related to the  $W$  and  $Z$  boson masses, its scale cannot be taken as an arbitrary parameter. However, thanks to the one-loop factor, the compactification scale becomes typically  $O(10 \text{ TeV})$ . Therefore, the gauge hierarchy problem is solved.

In a previous paper by the present authors, we have proposed a 2HDM in a 6D  $SU(4)$  gauge theory compactified on an orbifold  $T^2/Z_2$  with a fermion in a totally four symmetric tensor representation [18], which potentially solve the above mentioned problem. In addition, our tree-level quartic Higgs potential is obtained from the gauge kinetic term, which automatically has the  $Z_2$  symmetry and CP conservation because the coupling constant of the quartic Higgs potential is given by the gauge coupling. Moreover, a remarkable feature of  $SU(4)$  model predicts that the weak mixing angle at the compactification scale is  $\sin^2 \theta_W = 1/4$  [13], independent of the fermion matter content. As for fermions, we only

considered a massless 6D fermion in the  $\overline{\mathbf{35}}$  representation where a top quark is embedded as a zero mode after compactification. This is because the contribution from  $\overline{\mathbf{35}}$  to one-loop effective potential is dominant and those from the representations where fermions other than the top quark are embedded are exponentially suppressed by the 6D bulk mass effects. Although we found that the electroweak symmetry breaking is realized, unfortunately, the SM Higgs mass and the compactification scale are found to be small comparing the experimental data. However, it is known that introducing the brane-localized gauge kinetic terms (BLKTs) at the fixed points enhances the compactification scale [19].

In this paper, we introduce the BLKTs at the fixed points to our previous 2HDM model [18], reanalyze the Kaluza-Klein (KK) mode spectrum of the gauge field, and calculate the Higgs potential and the related Higgs mass spectrum. In particular, we investigate the electroweak symmetry breaking and the SM Higgs mass. We show that the electroweak symmetry is indeed broken at the potential minimum. As will be also shown later, the SM Higgs mass 125 GeV can be realized by an enhancement effect of the BLKT as expected. We also show the other predicted mass spectra of charged Higgs, CP-even Higgs and CP-odd Higgs.

This paper is organized as follows. In the next section, we explain our 2HDM model originated from a 6D  $SU(4)$  gauge theory. In section 3, we carefully calculate the KK mass of the gauge field in the presence of BLKTs. In section 4, the one-loop Higgs potential is calculated using the KK mass spectrums of the gauge field obtained in section 3 and a fermion in the  $\overline{\mathbf{35}}$  representation of  $SU(4)$ . We further discuss in section 5 the electroweak symmetry breaking, a possibility to obtain a realistic SM Higgs mass, and the other physical Higgs mass spectra. Summary is devoted to section 6. The detail calculation of section 3 is summarized in Appendix A.  $SU(4)$  generators are listed in Appendix B.

## 2 Setup

We consider a six-dimensional  $SU(4)$  GHU model compactified on the orbifold  $T^2/Z_2$ . Let us briefly explain why we employ this setup. In general, the weak mixing angle can be predicted when the SM hypercharge gauge group  $U(1)_Y$  is embedded into a simple gauge group. In the simplest GHU realization based on  $SU(3)$ , the SM Higgs doublet originates from the adjoint representation of the  $SU(3)$  gauge field. However, this minimal model is

known to predict  $\sin^2 \theta_W = 3/4$  at the compactification scale, which is phenomenologically unacceptable [4]. It was pointed out in [13] that a realistic weak mixing angle  $\sin^2 \theta_W = 1/4$  at the compactification scale (to be compared with the experimental value  $\sin^2 \theta_W \simeq 0.23$  at the electroweak scale), can be obtained if the SM Higgs doublet is embedded in a triplet or a sextet representation of an  $SU(3)$  subgroup. A smallest unitary group containing an  $SU(3)$  subgroup and accommodating these representations is  $SU(4)$ . In particular, the adjoint representation is decomposed as  $\mathbf{15} \rightarrow \mathbf{8} + \mathbf{3} + \bar{\mathbf{3}} + \mathbf{1}$  under  $SU(3)$  and the  $SU(3)$  triplets appear, which motivates our choice of the  $SU(4)$  gauge group.

In GHU, the Higgs doublets originate from extra dimensional components of higher-dimensional gauge fields. To realize a 2HDM within this framework, at least two extra dimensions are required. We therefore focus on the minimal six-dimensional case. In particular, a 2HDM like spectrum of zero mode can be obtained in the case of  $T^2/Z_2$  compactification [14]. We take the spacetime to be  $M^4 \times T^2/Z_2$ , where  $M^4$  is a four-dimensional Minkowski spacetime and  $T^2/Z_2$  is a square torus with common radius  $R$  modded out by the  $Z_2$  parity. By imposing the  $Z_2$  orbifold boundary conditions, a chiral spectrum is obtained in the four dimensional (4D) effective four-dimensional theory and the gauge symmetry can be broken.

In addition, we introduce the BLKTs at the orbifold fixed points. Such terms are generically induced by radiative corrections [19] even if they are absent at tree-level. The existence of the BLKTs can significantly affect the KK spectrum of the gauge field, consequently, the 4D effective Higgs potential. The effect of the BLKTs can be roughly understood as follows. As will be seen below, the 4D effective gauge coupling is modified by adding BLKTs, roughly  $\frac{1}{g_4^2} \rightarrow \frac{1+c}{g_4^2}$  where  $c$  is a coefficient of the BLKTs. This shift of the gauge coupling accordingly changes the  $W$  boson mass like (3.24), which means that the compactification scale  $1/R$  should be enhanced in order to keep  $W$  boson mass for  $c > 0$ . Since the SM Higgs mass is proportional to the compactification scale, the SM Higgs mass is also expected to be enhanced. Therefore, this effects will improve the small SM Higgs mass obtained in our previous paper as mentioned in the introduction.

We now specify the 6D Lagrangian. The gauge sector of the 6D Lagrangian and the

field strength are given by

$$\mathcal{L}_g = -\frac{1}{2} \text{Tr}(F^{MN} F_{MN}) - \frac{1}{2} \sum_i \{4\pi^2 R^2 c_i \delta(x^5 - x_i^5) \delta(x^6 - x_i^6)\} \text{Tr}(F^{\mu\nu} F_{\mu\nu}), \quad (2.1)$$

$$F_{MN} = \partial_M A_N - \partial_N A_M - ig[A_M, A_N], \quad (M, N = 0, 1, 2, 3, 5, 6, \mu, \nu = 0, 1, 2, 3). \quad (2.2)$$

The first term in (2.1) is the gauge kinetic term in the 6D bulk and the second ones are 4D BLKTs for unbroken gauge groups at the fixed points. Here  $c_i$  are dimensionless BLKT coefficients taken to be independent at different fixed points and the index  $i$  labels the fixed points as seen below. We employ the metric convention  $\eta_{MN} = \text{diag}(-1, +1, \dots, +1)$ , and  $g$  denoted the 6D gauge coupling with mass dimension  $-1$ . The extra dimensional coordinates are represented by  $(x^5, x^6)$  with  $x^5, x^6 \in [0, 2\pi R)$ .  $Z_2$  transformation  $(x^{5,6} \rightarrow -x^{5,6})$  gives the fundamental region of extra dimensions as  $x^5 \in [0, \pi R]$ ,  $x^6 \in [0, 2\pi R)$ .  $T^2/Z_2$  orbifold yields four fixed points invariant under the  $Z_2$ ,

$$(x_i^5, x_i^6) \in \{(0, 0), (0, \pi R), (\pi R, 0), (\pi R, \pi R)\}, \quad (i = 0, 1, 2, 3). \quad (2.3)$$

Since the extra dimensions are compactified, we must impose consistent boundary conditions for translations on  $T^2$  together with  $Z_2$  parity conditions around the fixed points. The general boundary conditions on  $T^2/Z_2$  were studied in detail [17]. For the translations on  $T^2$ , we impose

$$A_M(x^\mu, x^5 + 2\pi R, x^6) = U_5 A_M(x^\mu, x^5, x^6) U_5^\dagger, \quad (2.4)$$

$$A_M(x^\mu, x^5, x^6 + 2\pi R) = U_6 A_M(x^\mu, x^5, x^6) U_6^\dagger, \quad (2.5)$$

where  $U_{5,6}$  are constant unitary group elements specifying the boundary conditions and satisfy  $[U_5, U_6] = 0$ . The  $Z_2$  parity conditions for the 6D gauge fields around the fixed points are given by

$$A_\mu(x^\mu, x_i^5 - x^5, x_i^6 - x^6) = +P_i A_\mu(x^\mu, x_i^5 + x^5, x_i^6 + x^6) P_i^{-1}, \quad (2.6)$$

$$A_{5,6}(x^\mu, x_i^5 - x^5, x_i^6 - x^6) = -P_i A_{5,6}(x^\mu, x_i^5 + x^5, x_i^6 + x^6) P_i^{-1}, \quad (2.7)$$

where  $P_i$  ( $i = 0, 1, 2, 3$ ) are the parity matrices assigned to each fixed point. Consistency of the boundary conditions on  $T^2/Z_2$  implies the relations [17]

$$P_1 = U_5 P_0, \quad P_2 = U_6 P_0, \quad P_3 = U_6 U_5 P_0, \quad (2.8)$$

which implies only three parity matrices are independent ( $P_3 = P_1 P_0 P_2 = P_2 P_0 P_1$ ). In what follows, we choose

$$P_0 = P_1 = \text{diag}(+1, +1, +1, -1), \quad (2.9)$$

$$P_2 = P_3 = \text{diag}(+1, +1, -1, -1), \quad (2.10)$$

which breaks the  $SU(4)$  gauge symmetry to  $SU(2)_L \times U(1)_Y \times U(1)_X$  in the 4D effective theory. It is convenient to encode the parities under  $(P_0, P_2)$  by a pair of signs  $(\pm \pm)$  for each component of the fundamental representation. With this notation, we summarize the parity assignment as

$$P = \text{diag}((++), (++) , (+-), (--) ). \quad (2.11)$$

The  $Z_2$  parities of each component of the  $SU(4)$  gauge fields are obtained as

$$A_\mu : \left( \begin{array}{cc|cc} (++) & (++) & (+-) & (--) \\ (++) & (++) & (+-) & (--) \\ \hline (+-) & (+-) & (++) & (-+) \\ \hline (--) & (--) & (-+) & (++) \end{array} \right), \quad A_{5,6} : \left( \begin{array}{cc|cc} (--) & (--) & (-+) & (++) \\ (--) & (--) & (-+) & (++) \\ \hline (-+) & (-+) & (--) & (+-) \\ \hline (++) & (++) & (+-) & (--) \end{array} \right). \quad (2.12)$$

In particular, we note that the  $(++)$  components have four-dimensional massless modes. For  $A_\mu$ , the  $(++)$  corresponds to  $SU(2)_L \times U(1)_Y \times U(1)_X$  gauge fields in the low energy effective theory:

$$A_\mu \xrightarrow{\text{low-energy}} \begin{pmatrix} G_\mu & 0 \\ 0 & 0 \end{pmatrix} + X_\mu \frac{\sqrt{6}}{12} \text{diag}(1, 1, 1, -3), \quad (2.13)$$

$$G_\mu = \begin{pmatrix} \frac{1}{2}\gamma_\mu + \frac{\sqrt{3}}{6}Z_\mu & \frac{1}{\sqrt{2}}W_\mu^+ & 0 \\ \frac{1}{\sqrt{2}}W_\mu^- & -\frac{\sqrt{3}}{3}Z_\mu & 0 \\ 0 & 0 & -\frac{1}{2}\gamma_\mu + \frac{\sqrt{3}}{6}Z_\mu \end{pmatrix}. \quad (2.14)$$

For the extra-dimensional components  $A_5$  and  $A_6$ , the  $(++)$  modes are present in the off-diagonal blocks as  $SU(2)_L$  doublets. We identify these scalar degrees of freedom with two Higgs doublets,

$$A_{5,6} \xrightarrow{\text{low-energy}} \frac{1}{\sqrt{2}} \begin{pmatrix} 0 & 0 & 0 & \phi_{1,2}^+ \\ 0 & 0 & 0 & \phi_{1,2}^0 \\ 0 & 0 & 0 & 0 \\ \phi_{1,2}^- & \phi_{1,2}^{0*} & 0 & 0 \end{pmatrix}, \quad \Phi_{1,2} = \begin{pmatrix} \phi_{1,2}^+ \\ \phi_{1,2}^0 \end{pmatrix}. \quad (2.15)$$

As mentioned above, the Higgs doublets are embedded in  $SU(3)$  triplet under the  $SU(4)$  subgroup. Consequently, the weak mixing angle is predicted as  $\sin^2 \theta_W = 1/4$  at the compactification scale.

The tree-level Higgs potential is extracted from the commutator part in the gauge kinetic term (2.1):

$$\text{Tr} (F_{MN} F^{MN}) \supset (-ig)^2 \text{Tr} ([A_5, A_6]^2). \quad (2.16)$$

At tree-level, only quartic terms are present. Note that the local Higgs mass terms are forbidden by the higher-dimensional gauge invariance. A characteristic feature of GHU is that the quartic coupling is fixed by the gauge coupling, enhancing a predictability in the Higgs sector. Moreover, the tree-level potential is automatically CP invariant because it is determined by a real gauge coupling, which should be contrasted with the general 2HDM where the CP invariance is often assumed. Rewriting the tree-level potential in terms of the two Higgs doublets, we obtain

$$V_{\text{tree}}(\Phi_1, \Phi_2) = \frac{g_4^2}{2} \left[ (\Phi_1^\dagger \Phi_1)(\Phi_2^\dagger \Phi_2) + (\Phi_1^\dagger \Phi_2)(\Phi_2^\dagger \Phi_1) - (\Phi_2^\dagger \Phi_1)^2 - (\Phi_1^\dagger \Phi_2)^2 \right], \quad (2.17)$$

where  $g_4$  denotes the 4D gauge coupling. This potential corresponds to the cases  $m_{11}^2 = m_{22}^2 = m_{12}^2 = \lambda_{1,2,6,7} = 0, \lambda_{3,4} = \frac{g_4^2}{2}, \lambda_5 = -g_4^2$  of the general scalar potential of the ordinary 2HDM

$$\begin{aligned} V_{\text{tree}}(\Phi_1, \Phi_2) = & m_{11}^2 \Phi_1^\dagger \Phi_1 + m_{22}^2 \Phi_2^\dagger \Phi_2 + m_{12}^2 (\Phi_1^\dagger \Phi_2 + \text{h.c.}) \\ & + \frac{\lambda_1}{2} (\Phi_1^\dagger \Phi_1)^2 + \frac{\lambda_2}{2} (\Phi_2^\dagger \Phi_2)^2 + \lambda_3 (\Phi_1^\dagger \Phi_1)(\Phi_2^\dagger \Phi_2) + \lambda_4 (\Phi_1^\dagger \Phi_2)(\Phi_2^\dagger \Phi_1) \\ & + \left[ \frac{\lambda_5}{2} (\Phi_1^\dagger \Phi_2)^2 + \lambda_6 (\Phi_1^\dagger \Phi_1)(\Phi_1^\dagger \Phi_2) + \lambda_7 (\Phi_2^\dagger \Phi_2)(\Phi_1^\dagger \Phi_2) + \text{h.c.} \right]. \end{aligned} \quad (2.18)$$

Note that  $V_{\text{tree}}$  possesses a  $Z_2$  symmetry  $(\Phi_1, \Phi_2) \rightarrow (\Phi_1, -\Phi_2)$  or  $(\Phi_1, \Phi_2) \rightarrow (-\Phi_1, \Phi_2)$ . Although a softly broken  $Z_2$  symmetry is often imposed by hand to suppress tree-level FCNCs in the ordinary 2HDM, the  $Z_2$  symmetry is present at tree-level in our model and we will see that a soft-breaking mass term is generated at one-loop.

We parametrize the vacuum expectation values (VEVs) as

$$\langle \Phi_1 \rangle = \begin{pmatrix} 0 \\ \frac{v_1}{\sqrt{2}} \end{pmatrix}, \quad \langle \Phi_2 \rangle = \begin{pmatrix} 0 \\ \frac{v_2}{\sqrt{2}} \end{pmatrix}, \quad (v_1, v_2 \in \mathbb{R}). \quad (2.19)$$

Along this direction the tree-level potential is vanishing,  $V_{\text{tree}}(v_1, v_2) = 0$ , analogous to the  $D$ -flat direction in supersymmetric theories. Since the magnitudes of  $v_{1,2}$  are undetermined at tree-level, we must compute the one-loop effective potential to determine the vacuum and the mass spectrum.

### 3 KK spectrum

To compute the one-loop effective potential, it is convenient to parameterize the vacuum by Wilson-line phases along the two cycles of  $T^2$ . For constant zero modes backgrounds of  $A_5$ ,  $A_6$ , we define

$$W_5 \equiv \mathcal{P} \exp \left( ig \int_0^{2\pi R} dx^5 A_5 \right), \quad W_6 \equiv \mathcal{P} \exp \left( ig \int_0^{2\pi R} dx^6 A_6 \right), \quad (3.1)$$

and parameterize them by two Wilson-line phases  $\alpha_1$  and  $\alpha_2$ . These phases are related to the VEVs  $v_{1,2}$  as

$$\alpha_1 = gRv_1, \quad \alpha_2 = gRv_2. \quad (3.2)$$

The Wilson-line phases  $\alpha_{1,2}$  can be implemented as twists in the boundary conditions. Concretely, for a mode function  $f(x^5, x^6)$  we impose

$$f(x^5 + 2\pi R, x^6) = e^{i\pi m \alpha_1} f(x^5, x^6), \quad (3.3)$$

$$f(x^5, x^6 + 2\pi R) = e^{i\pi(m\alpha_2 + q)} f(x^5, x^6), \quad (3.4)$$

where  $m \in \mathbb{Z}$  labels the weight of the generator, and  $q = 0$  (1) corresponds to the periodic (anti-periodic) boundary condition. A convenient basis compatible with (3.3) and (3.4) is provided

$$f(x^5, x^6) = e^{i(\lambda_5 x^5 + \lambda_6 x^6)}, \quad \lambda_5 = \frac{n_1 + \frac{m\alpha_1}{2}}{R}, \quad \lambda_6 = \frac{n_2 + \frac{m\alpha_2 + q}{2}}{R}, \quad (n_1, n_2 \in \mathbb{Z}), \quad (3.5)$$

which yields the KK spectrum

$$M_{n_1, n_2}^2 = \frac{(n_1 + \frac{m\alpha_1}{2})^2 + (n_2 + \frac{m\alpha_2 + q}{2})^2}{R^2}, \quad (-\infty < n_1, n_2 < \infty). \quad (3.6)$$

### 3.1 Effect of BLKT on the mass equation

In the presence of BLKTs, the mode functions in the extra dimensions satisfy an eigenvalue equation with the localized terms. For a given KK mass  $M$ , the profile  $f(x^5, x^6)$  obeys

$$\left[ \partial_5^2 + \partial_6^2 + M^2 + 4\pi^2 M^2 R^2 \sum_{i=0}^3 c_i \delta(x^5 - x_i^5) \delta(x^6 - x_i^6) \right] f(x^5, x^6) = 0. \quad (3.7)$$

Equation (3.7) implies nontrivial conditions at the fixed points, and therefore the KK quantization is modified compared to the BLKT-free case.

To incorporate the background phases  $(\alpha_1, \alpha_2)$ , we expand  $f(x^5, x^6)$  in the basis of (3.5). As a result, the KK spectrum is determined by a coupled linear system for the coefficients, equivalently by a quantization condition for  $M$  that depends on the coefficient of the BLKTs. For  $M^2 \neq \lambda_5^2 + \lambda_6^2$ , one finds the solution as

$$f(x^5, x^6) = M^2 \sum_{i=0}^3 c_i f(x_i^5, x_i^6) \sum_{n_1, n_2 \in \mathbb{Z}} \frac{e^{-i(\lambda_5(x_i^5 - x^5) + \lambda_6(x_i^6 - x^6))}}{\lambda_5^2 + \lambda_6^2 - M^2}. \quad (3.8)$$

Evaluating this expression at the fixed points leads to the following system of equations:

$$\begin{pmatrix} 1 - M^2 c_0 S & -M^2 c_1 S_-^{(6)} & -M^2 c_2 S_-^{(5)} & -M^2 c_3 S_- \\ -M^2 c_0 S_+^{(6)} & 1 - M^2 c_1 S & -M^2 c_2 T_- & -M^2 c_3 S_-^{(5)} \\ -M^2 c_0 S_+^{(5)} & -M^2 c_1 T_+ & 1 - M^2 c_2 S & -M^2 c_3 S_-^{(6)} \\ -M^2 c_0 S_+ & -M^2 c_1 S_+^{(5)} & -M^2 c_2 S_+^{(6)} & 1 - M^2 c_3 S \end{pmatrix} \begin{pmatrix} f(0, 0) \\ f(0, \pi R) \\ f(\pi R, 0) \\ f(\pi R, \pi R) \end{pmatrix} = 0. \quad (3.9)$$

Here we have defined lattice sums evaluated with the twisted momenta  $\lambda_{5,6}$ ,

$$S = \sum_{n_1, n_2 \in \mathbb{Z}} \frac{1}{\lambda_5^2 + \lambda_6^2 - M^2}, \quad S_{\pm}^{(5)} = \sum_{n_1, n_2 \in \mathbb{Z}} \frac{e^{\pm i \lambda_5 \pi R}}{\lambda_5^2 + \lambda_6^2 - M^2}, \quad S_{\pm}^{(6)} = \sum_{n_1, n_2 \in \mathbb{Z}} \frac{e^{\pm i \lambda_6 \pi R}}{\lambda_5^2 + \lambda_6^2 - M^2},$$

$$S_{\pm} = \sum_{n_1, n_2 \in \mathbb{Z}} \frac{e^{\pm i(\lambda_5 + \lambda_6) \pi R}}{\lambda_5^2 + \lambda_6^2 - M^2}, \quad T_{\pm} = \sum_{n_1, n_2 \in \mathbb{Z}} \frac{e^{\pm i(\lambda_5 - \lambda_6) \pi R}}{\lambda_5^2 + \lambda_6^2 - M^2}.$$

Note that the number of equations corresponds to the number of fixed points. For example, in the case of  $S^1/Z_2$  or  $T^2/Z_4$ , we obtain two fixed points. Thus, the size of the matrix in (3.9) becomes  $2 \times 2$ .

For (3.9) to have a nontrivial solution, the determinant must vanish:

$$\det \begin{pmatrix} 1 - M^2 c_0 S & -M^2 c_1 S_-^{(6)} & -M^2 c_2 S_-^{(5)} & -M^2 c_3 S_- \\ -M^2 c_0 S_+^{(6)} & 1 - M^2 c_1 S & -M^2 c_2 T_- & -M^2 c_3 S_-^{(5)} \\ -M^2 c_0 S_+^{(5)} & -M^2 c_1 T_+ & 1 - M^2 c_2 S & -M^2 c_3 S_-^{(6)} \\ -M^2 c_0 S_+ & -M^2 c_1 S_+^{(5)} & -M^2 c_2 S_+^{(6)} & 1 - M^2 c_3 S \end{pmatrix} = 0. \quad (3.10)$$

Expanding (3.10) for small  $M \ll 1/R$ , the equation determining the zero-mode mass becomes

$$1 - (c_0 + c_1 + c_2 + c_3)M^2S + \mathcal{O}(M^4) = 0. \quad (3.11)$$

Here, we define the sum of the coefficients of the localized terms as

$$c \equiv c_0 + c_1 + c_2 + c_3. \quad (3.12)$$

In practice, the dominant contribution to the effective potential comes from the low lying KK mode. The mixing effects associated with localized terms at different fixed points (e.g. the term proportional to  $c_0c_1$ ) mainly appear in higher KK levels. For the  $M \ll 1/R$  case, the mixing effects are off-diagonal matrix elements in (3.10) and are higher order in  $M^2$ . This means that the determinant of the matrix is dominantly given by the product of the diagonal elements, which reduces to (3.11).

### 3.2 Shift of the mass spectrum

We examine the mass shift of the KK zero mode induced by the BLKT at the origin. For the single fixed-point case  $c_0 \equiv c$  and  $c_{1,2,3} = 0$ , the KK masses are determined by the quantization condition

$$1 - cM^2S(M; \alpha_1, \alpha_2) = 0. \quad (3.13)$$

Introducing the dimensionless variable  $x \equiv MR$  and using the twisted parameter, this condition can be written in the dimensionless form

$$1 - cx^2 \sum_{n_1, n_2 \in \mathbb{Z}} \frac{1}{\left(n_1 + \frac{m\alpha_1}{2}\right)^2 + \left(n_2 + \frac{m\alpha_2 + q}{2}\right)^2 - x^2} = 0. \quad (3.14)$$

For  $c = 0$ , the solutions reduce to the BLKT-free spectrum

$$x^2 = \left(n_1 + \frac{m\alpha_1}{2}\right)^2 + \left(n_2 + \frac{m\alpha_2 + q}{2}\right)^2, \quad (n_1, n_2 \in \mathbb{Z}). \quad (3.15)$$

We now turn to the case  $c > 0$ . We first evaluate the sum over  $n_2$  using the analytic continuation for the complex number  $\omega$

$$\sum_{n=-\infty}^{\infty} \frac{1}{(n + \alpha)^2 - \omega^2} = \frac{\pi}{\omega} \frac{\sin(2\pi\omega)}{\cos(2\pi\omega) - \cos(2\pi\alpha)}. \quad (3.16)$$

Defining  $z_{n_1} \equiv x^2 - \left(n_1 + \frac{m\alpha_1}{2}\right)^2$ , we obtain

$$S(M; \alpha_1, \alpha_2) = \begin{cases} \sum_{n_1} \frac{\pi R^2}{\sqrt{|z_{n_1}|}} \frac{\sin\left(2\pi\sqrt{|z_{n_1}|}\right)}{\cos\left(2\pi\sqrt{|z_{n_1}|}\right) - \cos(\pi(m\alpha_2 + q))}, & (z_{n_1} > 0), \\ \sum_{n_1} \frac{\pi R^2}{\sqrt{|z_{n_1}|}} \frac{\sinh\left(2\pi\sqrt{|z_{n_1}|}\right)}{\cosh\left(2\pi\sqrt{|z_{n_1}|}\right) - \cos(\pi(m\alpha_2 + q))}, & (z_{n_1} < 0), \end{cases} \quad (3.17)$$

$$= \sum_{n_1} \frac{\pi R^2}{\sqrt{z_{n_1}}} \frac{\sin\left(2\pi\sqrt{z_{n_1}}\right)}{\cos\left(2\pi\sqrt{z_{n_1}}\right) - \cos(\pi(m\alpha_2 + q))}, \quad (3.18)$$

where the branch of  $\sqrt{z_{n_1}}$  is chosen by analytic continuation. Substituting (3.18) into (3.14), the quantization condition becomes

$$1 - c\pi x^2 \sum_{n \in \mathbb{Z}} \frac{1}{\sqrt{z_n}} \frac{\sin\left(2\pi\sqrt{z_n}\right)}{\cos\left(2\pi\sqrt{z_n}\right) - \cos(\pi(m\alpha_2 + q))} = 0. \quad (3.19)$$

We focus on the solution continuously connected zero mode with  $(n_1, n_2) = (0, 0)$ . To this end, we remove the divergent part via infinite sums and examine the dominantly contributing part. We define the part within the sum as follows.

$$\mathcal{S}_n \equiv \frac{1}{\sqrt{z_n}} \frac{\sin\left(2\pi\sqrt{z_n}\right)}{\cos\left(2\pi\sqrt{z_n}\right) - \cos(\pi(m\alpha_2 + q))}. \quad (3.20)$$

The sum over  $\mathcal{S}_n$  exhibits a logarithmic divergence originating from the large  $|n|$  region, reflecting the asymptotic behavior  $\mathcal{S}_n \sim 1/|n|$ . We define a regulated combination by subtracting this universal asymptotics using the digamma function  $\psi(z)$ . Specifically, we introduce

$$\mathcal{S}_{\text{reg}}^{(m,q)} \equiv \mathcal{S}_0 + \lim_{N \rightarrow \infty} \left[ \sum_{n=1}^N (\mathcal{S}_n + \mathcal{S}_{-n}) - \psi\left(N + 1 + \frac{m\alpha_1}{2}\right) - \psi\left(N + 1 - \frac{m\alpha_1}{2}\right) \right]. \quad (3.21)$$

By this construction,  $\mathcal{S}_{\text{reg}}^{(m,q)}$  is finite.<sup>1</sup>

To check the validity of our regularization method discussed above, we approximately derive the  $W$  boson mass. Assuming  $\alpha_{1,2} \sim x \ll 1$ , the regularized remainder can be treated as an  $x$ -independent constant to leading order. Keeping only the dominant  $n = 0$  dependence, we approximate (3.19) as

$$1 - c\pi x^2 [\mathcal{S}_0(x; \alpha_1, \alpha_2) + 2\gamma] \simeq 0, \quad (3.22)$$

---

<sup>1</sup>Details are provided in Appendix A.

where  $\gamma = -\psi(1) \simeq 0.5772\dots$  is the Euler-Mascheroni constant. Discarding the  $x$ -independent divergent part which can be absorbed into a renormalization of the localized term and expand the  $n = 0$  term for  $x, \alpha_{1,2} \ll 1$ , we obtain the approximate solution for  $q = 0$

$$x^2 \simeq \frac{(m\alpha_1)^2 + (m\alpha_2)^2}{4(1+c)}. \quad (3.23)$$

As a result, for  $\alpha_{1,2} \ll 1$  the approximate  $W$  boson mass, corresponding to twisted parameter  $(m, q) = (1, 0)$ , is shifted as

$$M_W^2(c=0) = \frac{\alpha_1^2 + \alpha_2^2}{4R^2} \quad \Longrightarrow \quad M_W^2(c>0) \simeq \frac{\alpha_1^2 + \alpha_2^2}{4(1+c)R^2}. \quad (3.24)$$

Including BLKTs genuinely deforms the KK spectrum: the extra-dimensional wave functions obey boundary conditions at the fixed points, and the masses are determined by the determinant condition (3.10) rather than the simple shifted spectrum (3.6). For generic coefficients  $(c_0, c_1, c_2, c_3)$ , the spectrum depends not only on their magnitudes but also on how they are distributed among the fixed points, through the relative phases encoded in  $S_{\pm}^{(5,6)}$ ,  $S_{\pm}$ , and  $T_{\pm}$ . Nevertheless, the lightest mode relevant for the effective theory is non-degenerate, and expanding (3.10) at small  $M^2$  yields (3.11), showing that its leading shift depends only on  $c \equiv c_0 + c_1 + c_2 + c_3$ . This is consistent with the effective field theory viewpoint that, for a light state, localized kinetic terms mainly renormalize its wave function normalization at leading order, while information on the relative fixed point locations enters only beyond the leading low energy expansion. For higher mode, by contrast, the BLKT distribution can lift degeneracies and produce the mixing effects among different fixed points. However, these effects predominantly reshape the spectrum in the UV part of the KK tower, whose contribution to the effective potential is expected to be less important for the vacuum structure. Therefore, as a simplification, we adopt the single fixed point setup  $c_0 = c$ ,  $c_{1,2,3} = 0$ . This simplification retains the leading deformation of the lower KK spectrum that governs the vacuum structure, while avoiding unnecessary complications from the mixing effects of the fixed-points in the heavy sector.

## 4 One-loop effective potential

The one-loop effective potential is obtained by summing the vacuum energies of the KK towers in the background  $(\alpha_1, \alpha_2)$ . Denoting the BLKT-modified eigenvalues collectively

by  $M_k(m, q; \alpha_1, \alpha_2)$  where  $k$  labels the modified KK mass after imposing the twisted parameter, the contribution from a single real scalar degree of freedom to one-loop effective potential takes the standard form

$$V_{1\text{-loop}}^{(m,q)}(\alpha_1, \alpha_2) = \frac{1}{2} \sum_k \int \frac{d^4 p_E}{(2\pi)^4} \ln(p_E^2 + M_k^2(m, q; \alpha_1, \alpha_2)), \quad (4.1)$$

while fermion contributions are given by (4.1) multiplied by an overall  $(-1)$  factor and the spin degrees of freedom. We analyze the qualitative shape of the potential by substituting the dimensionless solution  $x_k \equiv RM_k$  obtained from the mass equation into the cutoff regularized representation of the effective potential,

$$V_{1\text{-loop}}^{(m,q)}(\alpha_1, \alpha_2) = -\frac{1}{32\pi^2 R^4} \sum_k \int_0^{(\Lambda R)^2} dl l e^{-x_k^2/l}, \quad (4.2)$$

where  $\Lambda$  is a cutoff scale. The full effective potential is obtained by summing (4.1) over all fields in the model with the appropriate multiplicities and with the corresponding assignments of  $(m, q)$  for each sector. In what follows, we evaluate

$$V_{\text{eff}}(m, q; \alpha_1, \alpha_2) = V_{\text{tree}}(\Phi_1, \Phi_2) + \sum_{(m,q)} V_{1\text{-loop}}^{(m,q)}(\alpha_1, \alpha_2), \quad (4.3)$$

which determines the vacuum  $(\alpha_1, \alpha_2)$ , and the Higgs spectrum is extracted. Using (3.2), the resulting effective potential can be equivalently expressed in terms of the Higgs VEVs  $(v_1, v_2)$ . To implement (4.2) in practice, we must determine, for each field component, the corresponding twist parameters  $(m, q)$  entering the KK spectrum. We begin with the  $SU(4)$  gauge fields and extract their BLKT-free eigenvalues, which allows us to identify the relevant  $(m, q)$  assignments before turning on BLKTs.

## 4.1 $SU(4)$ gauge fields

We now determine the KK spectrum of the  $SU(4)$  gauge fields in the background  $(\alpha_1, \alpha_2)$ , focusing first on the BLKT-free case in order to identify the twist parameters  $(m, q)$  for each component. Once  $(m, q)$  is fixed, the BLKT-modified masses  $M_k(m, q; \alpha_1, \alpha_2)$  follow from the quantization condition derived in the previous subsection and can be substituted into (4.2). The KK masses of the 4D gauge fields  $A_\mu^a$  originate from the covariant derivatives along the extra dimensions. From the gauge kinetic term, we extract

$$F_{\mu 5}^a F^{a\mu 5} \supset D_5 A_\mu^a D^5 A^{a\mu} = A_\mu^c [-(D_5^{cc'})^2] A_\mu^{c'}, \quad (4.4)$$

and similarly for the  $x^6$  direction. Accordingly, the KK mass operator acting on  $A_\mu$  is

$$\hat{M}^2 = -(D_5^2 + D_6^2), \quad (D_{5,6}^{ab} = \delta^{ab} \partial_{5,6} + ig f^{acb} A_{5,6}^c), \quad (4.5)$$

where the indices  $a, b, c$  label the  $SU(4)$  degrees of freedom and  $f^{abc}$  are the structure constant of  $SU(4)$ . We diagonalize  $\hat{M}^2$  in the adjoint representation using the generator basis  $T^a = t^a/2$  summarized in Appendix B. The Higgs VEVs originate from the  $(++)$  zero modes of  $A_{5,6}$ . In our convention (2.15), the background is taken along the generator  $T^{11}$ ,

$$\langle A_5^{11} \rangle = \frac{v_1}{\sqrt{2}}, \quad \langle A_6^{11} \rangle = \frac{v_2}{\sqrt{2}}. \quad (4.6)$$

Then the relevant mass mixing in (4.5) is controlled by the structure constants  $f^{a11b}$ . The non-vanishing entries needed for the mass matrix are

$$\begin{cases} f^{11110} = f^{61114} = f^{71113} = \frac{1}{2}, \\ f^{2119} = f^{31112} = -\frac{1}{2}, \\ f^{81112} = \frac{\sqrt{3}}{6}, f^{151112} = \sqrt{\frac{2}{3}}. \end{cases} \quad (4.7)$$

Diagonalizing the mass matrix with these structure constants, we obtain the BLKT-free mass eigenvalues. It is convenient to present them in a form that makes the correspondence to the spectrum (3.6) manifest:

$$M_{n_1, n_2}^2 = \frac{(n_1 + \frac{\alpha_1}{2})^2 + (n_2 + \frac{1}{2} + \frac{\alpha_2}{2})^2}{R^2} \times 2, \quad \frac{(n_1 + \frac{\alpha_1}{2})^2 + (n_2 + \frac{\alpha_2}{2})^2}{R^2} \times 2, \\ \frac{(n_1 + \alpha_1)^2 + (n_2 + \alpha_2)^2}{R^2} \times 1, \quad (-\infty < n_{1,2} < \infty). \quad (4.8)$$

where the degeneracy is explicitly specified for each eigenvalue.

Here the factors “2” or “1” in (4.8) indicate the degeneracies of the corresponding eigenvalues. Comparing with the universal form (3.6), we can immediately read off the twist assignments  $(m, q)$  for each tower: the shift  $(\alpha_1/2, \alpha_2/2)$  corresponds to  $(m, q) = (1, 0)$ , the shift  $(\alpha_1/2, \alpha_2/2 + 1/2)$  corresponds to  $(m, q) = (1, 1)$ , and the shift  $(\alpha_1, \alpha_2)$  corresponds to  $(m, q) = (2, 0)$ . These values of  $(m, q)$  will be used as inputs for the BLKT-modified quantization condition and, subsequently, for the one-loop effective potential.

Finally, since we are interested in the  $(\alpha_1, \alpha_2)$ -dependent part of the effective potential, we drop the  $\alpha_{1,2}$ -independent KK masses, which only contribute to an additive constant.

## 4.2 Fermions

We now discuss the fermionic contribution to the one-loop effective potential. In GHU, Yukawa interactions originate from the higher-dimensional gauge interaction  $g \bar{\Psi} \Gamma^{5,6} A_{5,6} \Psi$ . After compactification, four-dimensional Yukawa couplings are determined by overlap integral of zero mode wave functions of SM fermions. For fermions except for top quark, fermion masses are typically given by  $M_W e^{-MR}$ , where  $M_W, M$  are weak scale, six-dimensional fermion mass (referred as bulk mass), respectively. For top quark case, top quark mass can be realized if it is embedded into a 6D massless fermion in the four-rank totally symmetric tensor of the gauge group [19, 20]. On the other hand, one-loop effective potential from massive fermion contributions is known to be suppressed by a Boltzmann-like factor  $e^{-\pi MR}$ . Therefore, the most dominant contribution to one-loop effective potential is given by top quark, which will be calculated in detail. Since we assume that the BLKTs are absent in the fermion sector in this paper, the KK masses of fermions are given by the BLKT-free spectrum discussed below and can be used directly in the one-loop potential.

We impose the  $Z_2$  parity on a fermion in  $\overline{\mathbf{35}}$  representation as

$$\Psi_{jklm}(x_i^5 - x^5, x_i^6 - x^6) = -\mathcal{R}_{\overline{\mathbf{35}}}(P_i)(i\Gamma^5\Gamma^6)\Psi_{jklm}(x_i^5 + x^5, x_i^6 + x^6). \quad (4.9)$$

Here,  $j, k, l, m = 1, 2, 3, 4$  and 6D gamma matrices are given by

$$\Gamma^\mu = \begin{pmatrix} \gamma^\mu & \\ & \gamma^\mu \end{pmatrix}, \quad \Gamma^5 = \begin{pmatrix} & i\gamma^5 \\ i\gamma^5 & \end{pmatrix}, \quad \Gamma^6 = \begin{pmatrix} & \gamma^5 \\ -\gamma^5 & \end{pmatrix}, \quad (\mu = 0, 1, 2, 3) \quad (4.10)$$

where  $\gamma^\mu, \gamma^5$  are ordinary 4D gamma matrices. Since the Lagrangian for  $\Psi(\overline{\mathbf{35}})$  is

$$\mathcal{L}_f = \bar{\Psi}_{jklm}(i\Gamma^\mu D_\mu + i\Gamma^5 D_5 + i\Gamma^6 D_6)\Psi_{jklm}, \quad (4.11)$$

where the covariant derivative for a  $\overline{\mathbf{35}}$  representation fermion is

$$D_{5,6}\Psi_{jklm} = (\partial_{5,6}\delta_{jj'} + 4igA_{5,6}^a T_{jj'}^a)\Psi_{j'klm}. \quad (4.12)$$

The mass squared matrix of fermion is

$$\begin{aligned} \tilde{M}_{n_1, n_2}^2 &= (D_5\Gamma^5 + D_6\Gamma^6)^2 \\ &= M_{n_1, n_2}^2 + \frac{1}{2}\Gamma^5\Gamma^6[D_5, D_6] \\ &= M_{n_1, n_2}^2 + ig^2(I_4 \otimes \sigma_3)[A_5, A_6]. \end{aligned} \quad (4.13)$$

Noting that we consider the flat direction  $[A_5, A_6] = 0$ , the mass squared matrix of fermions takes the same form as that of  $SU(4)$  gauge fields.

Now, we decompose the  $\overline{\mathbf{35}}$  representation of  $SU(4)$  into  $SU(3)$  and  $SU(2)$  representations.

$$\begin{aligned}
\overline{\mathbf{35}} &\xrightarrow{SU(3)} \overline{\mathbf{15}}_{(++)} + \overline{\mathbf{10}}_{(+-)} + \overline{\mathbf{6}}_{(++)} + \overline{\mathbf{3}}_{(+-)} + \overline{\mathbf{1}}_{(++)} \\
&\xrightarrow{SU(2)} \mathbf{5}_{(++)} + \mathbf{4}_{(--)} + \mathbf{4}_{(+-)} + 2 \times \mathbf{3}_{(++)} + \mathbf{3}_{(-+)} \\
&\quad + 2 \times \mathbf{2}_{(--)} + 2 \times \mathbf{2}_{(+-)} + 5 \text{ singlets.}
\end{aligned} \tag{4.14}$$

In this decomposition, top quark is included as a zero mode in  $\overline{\mathbf{15}}$  representation of  $SU(3)$  [20]. More precisely, top quark corresponds to zero modes of  $\mathbf{2}_L$  and  $\mathbf{1}_R$  representations in the  $SU(2)$  decomposition of  $\overline{\mathbf{15}}$ . Note here that many massless exotic fermions appear from  $\overline{\mathbf{15}}$ ,  $\overline{\mathbf{6}}$  and  $\overline{\mathbf{1}}$  representations of  $SU(3)$ . Of these massless exotic fermions, those from  $SU(2)$  singlet give just constant contributions to one-loop effective potential since those are independent of Higgs VEV. Therefore, these are harmless. For other massless exotic fermions, they can be made massive by introducing four-dimensional Weyl fermions with the opposite chirality and conjugate representation on the brane at the fixed point and making Dirac mass terms with the massless exotic fermions. The mass of the exotic fermions obtained through the Dirac mass terms is also independent of Higgs VEV, therefore it is not necessary for one-loop effective potential to take into account their contributions.

From information (4.14), the KK mass spectrum of fermion in the  $\overline{\mathbf{35}}$  representation is obtained in the same way as the gauge field.

$$\begin{aligned}
\mathbf{5}_{(++)} &\rightarrow \frac{(n_1 + 2\alpha_1)^2 + (n_2 + 2\alpha_2)^2}{R^2}, \quad \frac{(n_1 + \alpha_1)^2 + (n_2 + \alpha_2)^2}{R^2}, \\
\mathbf{4}_{(--)} &\rightarrow \frac{(n_1 + \frac{3}{2}\alpha_1)^2 + (n_2 + \frac{3}{2}\alpha_2)^2}{R^2}, \quad \frac{(n_1 + \frac{1}{2}\alpha_1)^2 + (n_2 + \frac{1}{2}\alpha_2)^2}{R^2}, \\
\mathbf{4}_{(+-)} &\rightarrow \frac{(n_1 + \frac{3}{2}\alpha_1)^2 + (n_2 + \frac{1}{2} + \frac{3}{2}\alpha_2)^2}{R^2}, \quad \frac{(n_1 \pm \frac{1}{2}\alpha_1)^2 + (n_2 + \frac{1}{2} + \frac{1}{2}\alpha_2)^2}{R^2}, \\
\mathbf{3}_{(--)} &\rightarrow \frac{(n_1 + \alpha_1)^2 + (n_2 + \alpha_2)^2}{R^2}, \quad \mathbf{3}_{(-+)} \rightarrow \frac{(n_1 + \alpha_1)^2 + (n_2 + \frac{1}{2} + \alpha_2)^2}{R^2}, \\
\mathbf{2}_{(--)} &\rightarrow \frac{(n_1 + \frac{1}{2}\alpha_1)^2 + (n_2 + \frac{1}{2}\alpha_2)^2}{R^2}, \quad \mathbf{2}_{(+-)} \rightarrow \frac{(n_1 + \frac{1}{2}\alpha_1)^2 + (n_2 + \frac{1}{2} + \frac{1}{2}\alpha_2)^2}{R^2}
\end{aligned}$$

where  $n_{1,2}$  are integers.

### 4.3 Structure of the effective potential

The mass equation (3.19) is invariant under  $\alpha_{1,2} \rightarrow \alpha_{1,2} + 2$  for arbitrary  $m$ , and is symmetric under  $\alpha_{1,2} \rightarrow -\alpha_{1,2}$ . Therefore, without loss of generality, we may restrict the parameter region to  $0 \leq \alpha_{1,2} \leq 1$ . A further reduction of the fundamental region follows from the structure of the KK towers that appear in our model. For even  $m$ , the combination  $(m\alpha_2 + q)/2$  is invariant under  $\alpha_2 \rightarrow \alpha_2 + 1$  up to an integer shift, and hence each such tower is periodic with period 1 in the  $\alpha_2$  direction. For odd  $m$ , the spectrum with  $(m, q) = (m, 1)$  at a given  $\alpha_2$  is equivalent to that with  $(m, q) = (m, 0)$  at  $\alpha_2 + 1$ . Hence, if the effective potential contains an equal number of KK mode with  $(m, 0)$  and  $(m, 1)$  for odd  $m$ , their combined contribution is also periodic under  $\alpha_2 \rightarrow \alpha_2 + 1$ .

We list the assignments of the twist parameters  $(m, q)$  for the VEV-dependent KK mode in Table 1. From Table 1, we see that the VEV-dependent part of the potential in our model indeed contains the odd- $m$  pairs  $(m, 0)$  and  $(m, 1)$  with the same multiplicities (in particular for  $m = 1, 3$ ). Therefore the full potential is periodic with the period 1 in the  $\alpha_2$  direction. Combining this with the  $\alpha_2 \rightarrow -\alpha_2$  symmetry, we may take the fundamental region as

$$0 \leq \alpha_1 < 1, \quad 0 \leq \alpha_2 \leq \frac{1}{2}. \quad (4.15)$$

The plots of  $V_{\text{eff}}^{1\text{-loop}}$  are shown in Figure 1. A minimum point of the effective potential is found at  $\alpha_1^{\text{min}} \simeq 0.438$ ,  $\alpha_2^{\text{min}} \simeq 0.299$  as can be seen from Figure 1a. As will be discussed in the next section, the electroweak symmetry is broken to  $U(1)_{\text{em}}$  and an extra  $U(1)$  at the minimum. We find that the qualitative shape of the effective potential derived from the solutions of the mass equation is almost independent of the value of  $c$ . Moreover, even for  $c \sim \mathcal{O}(10)$ , electroweak symmetry breaking is confirmed.

$(m, q)$	$SU(4)$ gauge fields ( $c > 0$ )	$\overline{\mathbf{35}}$ fermion ( $c = 0$ )
(1, 0)	$SU(2)$ doublet ( $\times 2$ )	$\mathbf{2}_{(--)}(\times 2)$ and $\mathbf{4}_{(--)}$
(1, 1)	$SU(2)$ doublet ( $\times 2$ )	$\mathbf{2}_{(+-)}(\times 2)$ and $\mathbf{4}_{(+-)}$
(2, 0)	$SU(2)$ adjoint ( $\times 1$ )	$\mathbf{3}_{(++)}(\times 2)$ and $\mathbf{5}_{(++)}$
(2, 1)	–	$\mathbf{3}_{(-+)}$
(3, 0)	–	$\mathbf{4}_{(--)}$
(3, 1)	–	$\mathbf{4}_{(+-)}$
(4, 0)	–	$\mathbf{5}_{(++)}$

Table 1: Assignments of the twist parameters  $(m, q)$  for the VEV-dependent KK mode

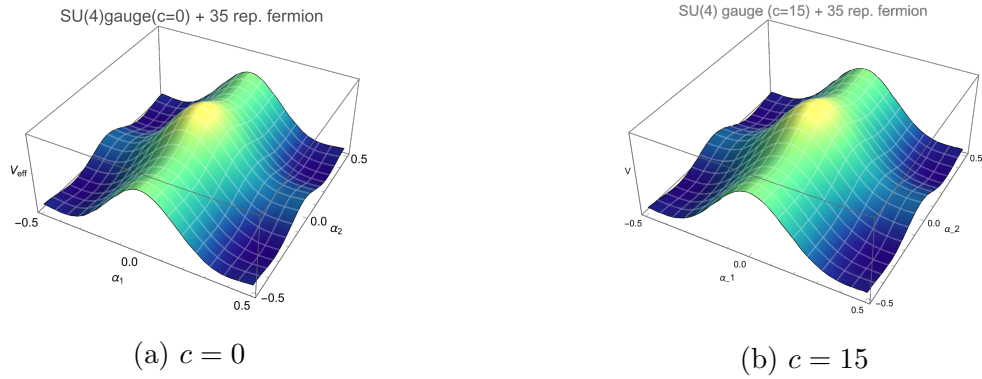


Figure 1: The shape of the effective potential. The potentials with (a)  $c = 0$  and (b)  $c = 15$  have a minimum at  $(\alpha_1^{\min}, \alpha_2^{\min}) = (0.44, 0.30)$  and  $(\alpha_1^{\min}, \alpha_2^{\min}) = (0.46, 0.30)$ , respectively.

## 5 Electroweak symmetry breaking

In this section, we discuss the pattern of electroweak symmetry breaking in our model and calculate the Higgs mass spectrum. In GHU, the physical order parameters are the Wilson-lines along the compact cycles. A corresponding gauge symmetry remains unbroken in the vacuum if the generator commutes with the VEV of the Wilson-line

$$\begin{aligned}
\langle W_{5,6} \rangle &= \mathcal{P} \exp \left[ ig \oint_{S^1} dx^{5,6} \langle A_{5,6} \rangle \right] \\
&= \begin{pmatrix} 1 & 0 & 0 & 0 \\ 0 & \cos(2\pi\alpha_{1,2}) & 0 & i \sin(2\pi\alpha_{1,2}) \\ 0 & 0 & 1 & 0 \\ 0 & i \sin(2\pi\alpha_{1,2}) & 0 & \cos(2\pi\alpha_{1,2}) \end{pmatrix}. \tag{5.1}
\end{aligned}$$

Conversely, the generators that do not commute with  $\langle W_{5,6} \rangle$  correspond to the broken generators, whose gauge bosons obtain masses via Higgs mechanism. The symmetry breaking patterns can be classified into the following three cases.

(i)  $\alpha_{1,2}^{\min} = 0$

$$\langle W_{5,6} \rangle = I_4. \quad (5.2)$$

In this case  $\langle W_{5,6} \rangle$  is a  $4 \times 4$  identity matrix  $I_4$ , which commutes with all generators of  $SU(4)$ . Therefore no additional breaking occurs beyond the orbifold reduction:

$$SU(4) \xrightarrow{Z_2 \text{ orbifold}} SU(2)_L \times U(1)_Y \times U(1)_X \quad (5.3)$$

(ii)  $\alpha_{1,2}^{\min} = \frac{1}{2}$

$$\langle W_{5,6} \rangle = \text{diag}(+1, -1, +1, -1). \quad (5.4)$$

Since  $\langle W_{5,6} \rangle$  is diagonal, it is commutative with the diagonal generators of  $SU(4)$ , namely  $T^3$ ,  $T^8$  and  $T^{15}$ :

$$[\langle W_{5,6} \rangle, T^3] = [\langle W_{5,6} \rangle, T^8] = [\langle W_{5,6} \rangle, T^{15}] = 0. \quad (5.5)$$

Thus,  $SU(2)_L$  is broken to  $U(1)$  and only three  $U(1)$  symmetries remain:

$$SU(4) \xrightarrow{Z_2 \text{ orbifold}} SU(2)_L \times U(1)_Y \times U(1)_X \xrightarrow{\text{quantum effect}} U(1) \times U(1)_Y \times U(1)_X. \quad (5.6)$$

(iii)  $0 < \alpha_{1,2}^{\min} < 1$ ,  $\alpha_{1,2}^{\min} \neq \frac{1}{2}$

In this case,  $\langle W_{5,6} \rangle$  has off-diagonal components. We find that the following commutation relations do not commute with all electroweak generators.

$$\begin{aligned} [\langle W_{5,6} \rangle, T^3] &= -\sin(2\pi\alpha_{1,2}^{\min})T^{12}, & [\langle W_{5,6} \rangle, T^8] &= \frac{\sin(2\pi\alpha_{1,2}^{\min})}{\sqrt{3}}T^{12}, \\ [\langle W_{5,6} \rangle, T^{15}] &= \frac{4\sin(2\pi\alpha_{1,2}^{\min})}{\sqrt{6}}T^{12}. \end{aligned} \quad (5.7)$$

This implies that only specific linear combinations of  $T^3, T^8, T^{15}$  remain unbroken. In particular, the electromagnetic generator

$$T_{\text{em}} = \frac{1}{2}T^3 + \frac{\sqrt{3}}{2}T^8 \quad (5.8)$$

commutes with  $\langle W_{5,6} \rangle$ , and the symmetry breaking pattern is SM-like:

$$SU(4) \xrightarrow{Z_2 \text{ orbifold}} SU(2)_L \times U(1)_Y \times U(1)_X \xrightarrow{\text{quantum effect}} U(1)_{em} \times U(1)'. \quad (5.9)$$

Here, the unbroken generator  $U(1)'$  is defined as  $T' = \frac{1}{\sqrt{2}}T^3 - \frac{1}{\sqrt{6}}T^8 + \frac{1}{\sqrt{3}}T^{15}$ .

Since the  $U(1)'$  gauge boson is massless as it stands, we propose the way to provide it a mass. We introduce a brane localized 4D scalar field which is assumed to be a gauge singlet  $\phi$  except for nonvanishing  $U(1)'$  charge and the Lagrangian is given by

$$\mathcal{L}_{\text{scalar}} = \delta(x^5 - x_i^5)\delta(x^6 - x_i^6) \left[ (D_\mu \phi)^*(D^\mu \phi) - \frac{\lambda}{4}(\phi^* \phi - V^2)^2 \right], \quad (5.10)$$

where  $\lambda$  is assumed to be real and positive, and the  $V$  is a VEV for  $\phi$ . The covariant derivative is with respect to  $U(1)'$  gauge group. Thus, the  $U(1)'$  is spontaneously broken and its gauge boson becomes massive. Here, we need to assume that the  $U(1)'$  gauge boson mass is in a range from the weak scale to at most the compactification scale for our analysis so far to remain unchanged.

## 5.1 Higgs mass

The scalar masses are obtained from the quadratic terms of the potential expanded around the vacuum. The two Higgs doublets originating from the extra-dimensional gauge components are parameterized as

$$\Phi_1 = \begin{pmatrix} \phi_1^+ \\ \frac{v_1 + h_1 + i\omega_1}{\sqrt{2}} \end{pmatrix}, \quad \Phi_2 = \begin{pmatrix} \phi_2^+ \\ \frac{v_2 + h_2 + i\omega_2}{\sqrt{2}} \end{pmatrix}, \quad (5.11)$$

where  $\phi_{1,2}^+$  are complex scalar fields and  $h_{1,2}$  and  $\omega_{1,2}$  are real scalar fields. The effective potential can be written as  $V_{\text{eff}}(\Phi_1, \Phi_2) = V_{\text{tree}} + V_{1\text{-loop}}$ ,

$$V_{\text{tree}} = \frac{g_4^2}{2} \left\{ (\Phi_1^\dagger \Phi_1)(\Phi_2^\dagger \Phi_2) + (\Phi_1^\dagger \Phi_2)(\Phi_2^\dagger \Phi_1) - (\Phi_1^\dagger \Phi_2)^2 - (\Phi_2^\dagger \Phi_1)^2 \right\}, \quad (5.12)$$

and the radiatively generated mass terms are parameterized as

$$V_{1\text{-loop}} = m_{11}^2(\Phi_1^\dagger \Phi_1) + m_{22}^2(\Phi_2^\dagger \Phi_2) - m_{12}^2(\Phi_1^\dagger \Phi_2 + \Phi_2^\dagger \Phi_1). \quad (5.13)$$

The vacuum  $(\alpha_1^{\min}, \alpha_2^{\min})$  is determined by minimizing  $V_{1\text{-loop}}$ . The relation between the curvature of the potential at the vacuum and the Higgs masses is given by

$$m_{ij}^2 = g_4^2 R^2 \left. \frac{\partial^2 V_{1\text{-loop}}}{\partial \alpha_i \partial \alpha_j} \right|_{\alpha_1^{\min}, \alpha_2^{\min}}. \quad (5.14)$$

Expanding  $V_{\text{eff}}(\Phi_1, \Phi_2)$  to quadratic order in fluctuations, the charged sector, CP-odd sector and CP-even sector of the Higgs potential take the following form

$$\begin{aligned}
V_{\text{eff}}(\Phi_1, \Phi_2) \supset & \left\{ m_{12}^2 + \frac{g_4^2 v_1 v_2}{4} \right\} \begin{pmatrix} \phi_1^- & \phi_2^- \end{pmatrix} \begin{pmatrix} \frac{v_2}{v_1} & -1 \\ -1 & \frac{v_1}{v_2} \end{pmatrix} \begin{pmatrix} \phi_1^+ \\ \phi_2^+ \end{pmatrix} \\
& + \frac{1}{2} \{ m_{12}^2 + g_4^2 v_1 v_2 \} \begin{pmatrix} \omega_1 & \omega_2 \end{pmatrix} \begin{pmatrix} \frac{v_2}{v_1} & -1 \\ -1 & \frac{v_1}{v_2} \end{pmatrix} \begin{pmatrix} \omega_1 \\ \omega_2 \end{pmatrix} \\
& + \frac{1}{2} \begin{pmatrix} h_1 & h_2 \end{pmatrix} \begin{pmatrix} m_{11}^2 & -m_{12}^2 \\ -m_{21}^2 & m_{22}^2 \end{pmatrix} \begin{pmatrix} h_1 \\ h_2 \end{pmatrix}. \tag{5.15}
\end{aligned}$$

Diagonalizing the above mass matrices for  $(\phi_1^\pm, \phi_2^\pm)$ ,  $(\omega_1, \omega_2)$ ,  $(h_1, h_2)$  into the mass eigenstate  $(G^\pm, h^\pm)$ ,  $(G^0, A^0)$ ,  $(h, \tilde{h})$ , respectively, we obtain the mass eigenvalues as follows.

$$\text{charged sector} : \begin{cases} M_{G^\pm}^2 = 0 \\ M_{h^\pm}^2 = \frac{g_4^2(v_1^2 + v_2^2)}{4} + \frac{m_{12}^2(v_1^2 + v_2^2)}{v_1 v_2} \end{cases} \tag{5.16}$$

$$\text{CP-odd sector} : \begin{cases} M_{G^0}^2 = 0 \\ M_{A^0}^2 = g_4^2(v_1^2 + v_2^2) + \frac{m_{12}^2(v_1^2 + v_2^2)}{v_1 v_2} \end{cases} \tag{5.17}$$

$$\text{CP-even sector} : \begin{cases} M_h^2 = \frac{1}{2} \left( m_{11}^2 + m_{22}^2 - \sqrt{(m_{11}^2 - m_{22}^2)^2 + 4m_{12}^4} \right) \\ M_{\tilde{h}}^2 = \frac{1}{2} \left( m_{11}^2 + m_{22}^2 + \sqrt{(m_{11}^2 - m_{22}^2)^2 + 4m_{12}^4} \right) \end{cases} \tag{5.18}$$

Here, the mixing angle between  $(\phi_1^\pm, \phi_2^\pm)$  and  $(G^\pm, h^\pm)$  or  $(\omega_1, \omega_2)$  and  $(G^0, A^0)$  are determined by  $\beta$  with  $\tan \beta = v_2/v_1 = \alpha_2/\alpha_1$ <sup>2</sup> while the mixing angle  $\alpha$  between the  $h_{1,2}$  and  $h, \tilde{h}$  is undetermined and labeled by  $\alpha$ . According to the current experiment,  $\beta - \alpha = \pi/2$  is strongly favored, called alignment limit [3]. Hereafter, we fix  $\beta - \alpha = \pi/2$ . From this alignment limit, we can identify  $h$  with SM higgs boson.

Using the relation

$$M_W^2 = \frac{(\alpha_1^{\min})^2 + (\alpha_2^{\min})^2}{4(1+c)R^2} = (80.4 \text{ GeV})^2, \tag{5.19}$$

---

<sup>2</sup>In the case of a torus with  $R_{1,2}$ ,  $\tan \beta$  is determined as  $\tan \beta = R_1 \alpha_2 / R_2 \alpha_1$ . Even if  $\alpha_2/\alpha_1 \lesssim 1$  is obtained,  $\tan \beta$  with  $R_1/R_2 \gtrsim 1$  would be expected to be large, which is favored for Type-I model [21,22].

we can rewrite the charged scalar mass and CP-odd scalar mass as

$$M_{h^\pm}^2 = (1+c)M_W^2 + \frac{m_{12}^2}{\sin\beta\cos\beta}, \quad M_{A^0}^2 = 4(1+c)M_W^2 + \frac{m_{12}^2}{\sin\beta\cos\beta}. \quad (5.20)$$

Both  $h^\pm$  and  $A^0$  are parametrically heavier than the weak scale  $M_W$ , and the localized kinetic term provides an efficient handle to raise their masses through the overall factor  $(1+c)$  at fixed  $M_W$  (5.19). This is consistent with the KK spectrum analysis: the BLKT effectively rescales the light-mode normalization and suppresses the Wilson-line induced gauge-boson mass, which in turn shifts the scalar spectrum when expressed in terms of the physical  $M_W$ . The CP-even sector contains two neutral scalars. One of them must reproduce the observed SM Higgs boson mass  $m_h \simeq 125$  GeV. In this framework,  $m_h$  is controlled by the curvature of the one-loop effective potential at  $(\alpha_1^{\min}, \alpha_2^{\min})$ . Consequently, the mass of the SM Higgs boson can be determined by the BLKT coefficient  $c$ . In Figure 2, we plot the CP even scalar masses vs. the BLKT coefficient  $c$ . The yellow and blue lines are the lighter and heavier scalar masses, respectively. The red dashed line indicates the observed SM Higgs mass. We find that the SM Higgs boson mass is realized by taking  $c \simeq 15$  and the compactification scale becomes 1.4 TeV. The second Higgs boson  $\tilde{h}$  has a mass for  $M_{\tilde{h}} \sim 227$  GeV.

Other physical Higgs masses can be predicted as

$$M_{h^\pm} \sim 330 \text{ GeV}, \quad M_{A^0} \sim 645 \text{ GeV}. \quad (5.21)$$

From the result of measurement of  $b \rightarrow s\gamma$ , the lower bound on the charged Higgs mass has known  $M_{h^\pm} > 580$  GeV in Type-II and Type-Y models, which is independent of  $\tan\beta$  [21,22]. Therefore, our model is excluded in Type-II and Type-Y models. We have to construct Yukawa sector of Type-I or Type-X models and study various phenomenology and the predictions in our model.

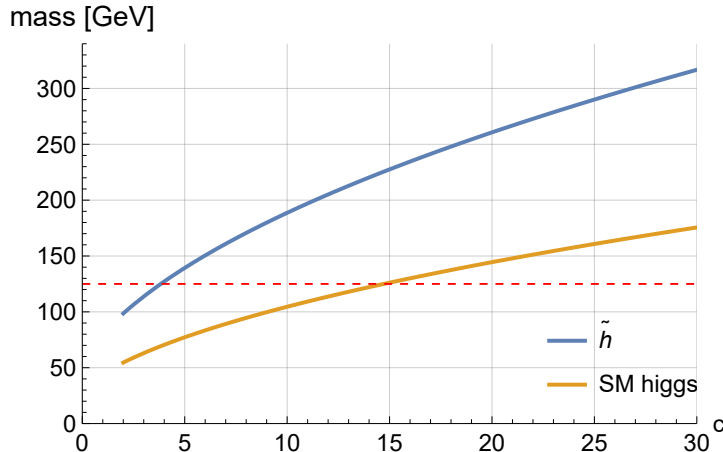


Figure 2: SM Higgs and the second Higgs masses as functions of the size of the BLKTs  $c$

## 6 Summary

In this paper, we have improved our previous proposed 2HDM originated from a 6D  $SU(4)$  gauge theory compactified on an orbifold  $T^2/Z_2$  by introducing the BLKTs at the fixed points. Two Higgs scalar fields are identified as the massless zero modes of extra components of the gauge field in our model. Therefore, the scalar fields are not need to be introduced by hand and built in our model. In this scenario called gauge-Higgs unification, it is well known that the gauge hierarchy problem is solved by the higher-dimensional gauge symmetry. In the ordinary 2HDM, this important issue remains unsolved. This  $SU(4)$  theory remarkably predicts the weak mixing angle at the compactification scale as  $\sin^2 \theta_W = 1/4$ . Since our Higgs sector is controlled by the 6D gauge symmetry, the form of Higgs potential is restricted in contrast to that in the ordinary 2HDM. Advantages of Higgs potential in our 2HDM compared to that of the ordinary 2HDM are CP invariance because of the gauge coupling for the coupling constant of the Higgs potential, incorporating automatically a  $Z_2$  symmetry to avoid FCNC, and softly broken  $Z_2$  symmetry terms are radiatively generated at one-loop. These properties of Higgs potential are simply assumed in the ordinary 2HDM. In our previous paper [18], we have studied the electroweak symmetry breaking and the SM Higgs mass in the same model of the present paper without the BLKTs. Although the electroweak symmetry breaking could be realized, the SM Higgs mass or equivalently the compactification scale were found to be

slightly small. We have reanalyzed these issues in the presence of the BLKTs and found that the SM Higgs mass 125 GeV can be obtained by the enhancement effect of BLKTs as well as the electroweak symmetry breaking is realized. Furthermore, other physical Higgs scalar mass spectrum were predicted.

As mentioned in the previous section, our Higgs mass spectrum are excluded in Type-II and Type-Y models since the charged Higgs boson mass is smaller than the experimental lower bound. Therefore, Type-I or Type-X models should be considered in Yukawa sector in our 2HDM and its phenomenology will be studied. In the present paper, the square torus compactification was considered for simplicity. It would be interesting to extend to more general torus compactification and study whether some impacts on the electroweak symmetry breaking and the Higgs mass spectrum can be obtained in such a compactification. These issues are left for our future work.

## Acknowledgments

This work was supported by Japan Society for the Promotion of Science, Grants-inAid for Scientific Research, No. JP25K07304 (N.M.), and JST SPRING, Grant Number JPMJSP2139 (K.A. and A.N.), and KSU Fundamental Research Fund in Kyshu Sangyo University, K024023 (T.H.).

## A Digamma Regularlization

In this appendix, we explain how the digamma subtraction used in Sec. 3.2 regularizes the logarithmic divergence of the analytically continued one-dimensional sum that appears after performing one of the KK sums. We consider the quantization condition (for  $c \neq 0$ )

$$1 - c\pi x^2 \sum_{n=-\infty}^{\infty} \mathcal{S}_n = 0, \quad (\text{A.1})$$

where

$$\mathcal{S}_n \equiv \frac{1}{\sqrt{x^2 - (n + \alpha_2)^2}} \frac{\sin\left(2\pi\sqrt{x^2 - (n + \alpha_2)^2}\right)}{\cos\left(2\pi\sqrt{x^2 - (n + \alpha_2)^2}\right) - \cos(2\pi\alpha_1)}. \quad (\text{A.2})$$

We are interested in approximate real solutions with  $x \lesssim \mathcal{O}(10)$ , since higher modes give a subdominant contribution to the effective potential. Let  $N$  be a sufficiently large integer satisfying  $x^2 \ll N^2$ . We split the sum as

$$\sum_{n=-\infty}^{\infty} \mathcal{S}_n = \mathcal{S}_0 + \sum_{n=1}^N (\mathcal{S}_n + \mathcal{S}_{-n}) + \sum_{n=N+1}^{\infty} (\mathcal{S}_n + \mathcal{S}_{-n}). \quad (\text{A.3})$$

For  $n \gg x$ , the square root becomes imaginary and the trigonometric functions turn into hyperbolic ones. In this regime, the denominator in (A.2) is dominated by  $\cosh(\dots)$ , and the dependence on  $\alpha_1$  becomes negligible. Using  $\tanh(2\pi n) \sim 1$  for large  $n$ , one finds the asymptotic behavior

$$\sum_{n=-N+1}^{\infty} \mathcal{S}_n \simeq \sum_{n=N+1}^{\infty} \frac{\tanh(2\pi(n + \alpha_1))}{n + \alpha_1} \quad (\text{A.4})$$

$$\simeq \sum_{n=N+1}^{\infty} \frac{1}{n + \alpha_1} \quad (\text{A.5})$$

Therefore the third term in (A.3) contains a logarithmic divergence:

$$\sum_{n=N+1}^{\infty} (\mathcal{S}_n + \mathcal{S}_{-n}) \sim \sum_{n=N+1}^{\infty} \left( \frac{1}{n + \alpha} + \frac{1}{n - \alpha} \right). \quad (\text{A.6})$$

The key point is that this divergence originates from the large- $n$  region and is essentially independent of  $x$  for fixed  $x \ll N$ .

To regularize the logarithmic divergence, we subtract the asymptotic terms in (A.5) and express the subtraction in terms of the digamma function. Recall that the digamma function is defined by

$$\psi(z) \equiv \frac{d}{dz} \ln \Gamma(z), \quad \psi(1) = -\gamma, \quad (\text{A.7})$$

where  $\gamma \simeq 0.5772\dots$  is the Euler-Mascheroni constant. It admits the representation

$$\psi(z) = \lim_{N \rightarrow \infty} \left\{ \log N - \sum_{k=0}^N \frac{1}{z+k} \right\}, \quad \psi(z+n) = \psi(z) + \sum_{k=1}^n \frac{1}{k+z-1}. \quad (\text{A.8})$$

From (A.8), for fixed  $N$  we obtain

$$\lim_{N' \rightarrow \infty} \left[ \sum_{n=N+1}^{N'} \frac{1}{n + \alpha_2} - \log N' \right] = -\psi(N + 1 + \alpha_2), \quad (\text{A.9})$$

$$\lim_{N' \rightarrow \infty} \left[ \sum_{n=N+1}^{N'} \frac{1}{n - \alpha_2} - \log N' \right] = -\psi(N + 1 - \alpha_2). \quad (\text{A.10})$$

Adding these expressions yields the regularized tail:

$$\begin{aligned} \lim_{N' \rightarrow \infty} \left[ \sum_{n=N+1}^{N'} \left( \frac{1}{n + \alpha_2} + \frac{1}{n - \alpha_2} \right) - 2 \log N' \right] \\ = -\psi(N + 1 + \alpha_2) - \psi(N + 1 - \alpha_2) \end{aligned} \quad (\text{A.11})$$

Using (A.11), we define the regularized sum as

$$\sum_{n=-\infty}^{\infty} \mathcal{S}_n \longrightarrow \mathcal{S}_0 + \sum_{n=1}^N (\mathcal{S}_n + \mathcal{S}_{-n}) - \psi(N + 1 + \alpha) - \psi(N + 1 - \alpha), \quad (\text{A.12})$$

which is finite for any fixed  $N$  with  $x \ll N$  and captures the  $x$ -dependent part relevant to the low-lying spectrum.

Substituting (A.12) into (A.1), we obtain the regularized quantization condition

$$1 - c\pi x^2 \left[ \mathcal{S}_0 + \sum_{n=1}^N (\mathcal{S}_n + \mathcal{S}_{-n}) - \psi(N + 1 + \alpha) - \psi(N + 1 - \alpha) \right] = 0. \quad (\text{A.13})$$

In the main text, we take  $N$  sufficiently large compared to the solution of interest so that the remaining  $N$ -dependence is numerically negligible.

## B $SU(4)$ generators

In this appendix,  $SU(4)$  generators  $T^a = t^a/2$  are summarized as follows.

$$\begin{aligned}
 t^1 &= \begin{pmatrix} 0 & 1 & 0 & 0 \\ 1 & 0 & 0 & 0 \\ 0 & 0 & 0 & 0 \\ 0 & 0 & 0 & 0 \end{pmatrix}, \quad t^2 = \begin{pmatrix} 0 & -i & 0 & 0 \\ i & 0 & 0 & 0 \\ 0 & 0 & 0 & 0 \\ 0 & 0 & 0 & 0 \end{pmatrix}, \quad t^3 = \begin{pmatrix} 1 & 0 & 0 & 0 \\ 0 & -1 & 0 & 0 \\ 0 & 0 & 0 & 0 \\ 0 & 0 & 0 & 0 \end{pmatrix}, \\
 t^4 &= \begin{pmatrix} 0 & 0 & 1 & 0 \\ 0 & 0 & 0 & 0 \\ 1 & 0 & 0 & 0 \\ 0 & 0 & 0 & 0 \end{pmatrix}, \quad t^5 = \begin{pmatrix} 0 & 0 & -i & 0 \\ 0 & 0 & 0 & 0 \\ i & 0 & 0 & 0 \\ 0 & 0 & 0 & 0 \end{pmatrix}, \\
 t^6 &= \begin{pmatrix} 0 & 0 & 0 & 0 \\ 0 & 0 & 1 & 0 \\ 0 & 1 & 0 & 0 \\ 0 & 0 & 0 & 0 \end{pmatrix}, \quad t^7 = \begin{pmatrix} 0 & 0 & 0 & 0 \\ 0 & 0 & -i & 0 \\ 0 & i & 0 & 0 \\ 0 & 0 & 0 & 0 \end{pmatrix}, \quad t^8 = \frac{1}{\sqrt{3}} \begin{pmatrix} 1 & 0 & 0 & 0 \\ 0 & 1 & 0 & 0 \\ 0 & 0 & -2 & 0 \\ 0 & 0 & 0 & 0 \end{pmatrix}, \\
 t^9 &= \begin{pmatrix} 0 & 0 & 0 & 1 \\ 0 & 0 & 0 & 0 \\ 0 & 0 & 0 & 0 \\ 1 & 0 & 0 & 0 \end{pmatrix}, \quad t^{10} = \begin{pmatrix} 0 & 0 & 0 & -i \\ 0 & 0 & 0 & 0 \\ 0 & 0 & 0 & 0 \\ i & 0 & 0 & 0 \end{pmatrix}, \quad t^{11} = \begin{pmatrix} 0 & 0 & 0 & 0 \\ 0 & 0 & 0 & 1 \\ 0 & 0 & 0 & 0 \\ 0 & 1 & 0 & 0 \end{pmatrix}, \quad t^{12} = \begin{pmatrix} 0 & 0 & 0 & 0 \\ 0 & 0 & 0 & -i \\ 0 & 0 & 0 & 0 \\ 0 & i & 0 & 0 \end{pmatrix}, \\
 t^{13} &= \begin{pmatrix} 0 & 0 & 0 & 0 \\ 0 & 0 & 0 & 0 \\ 0 & 0 & 0 & 1 \\ 0 & 0 & 1 & 0 \end{pmatrix}, \quad t^{14} = \begin{pmatrix} 0 & 0 & 0 & 0 \\ 0 & 0 & 0 & 0 \\ 0 & 0 & 0 & -i \\ 0 & 0 & i & 0 \end{pmatrix}, \quad t^{15} = \frac{1}{\sqrt{6}} \begin{pmatrix} 1 & 0 & 0 & 0 \\ 0 & 1 & 0 & 0 \\ 0 & 0 & 1 & 0 \\ 0 & 0 & 0 & -3 \end{pmatrix}.
 \end{aligned}$$

These generators satisfy an orthonormal condition,  $\text{Tr}[T^a T^b] = \delta_{ab}/2$ .

## References

- [1] G. C. Branco, P. M. Ferreira, L. Lavoura, M. N. Rebelo, M. Sher and J. P. Silva, “Theory and phenomenology of two-Higgs-doublet models,” *Phys. Rept.* **516**, 1-102 (2012); [arXiv:1106.0034 [hep-ph]].
- [2] J. Haller, A. Hoecker, R. Kogler, K. Mönig, T. Peiffer and J. Stelzer, “Update of the global electroweak fit and constraints on two-Higgs-doublet models,” *Eur. Phys. J. C* **78**, no.8, 675 (2018); [arXiv:1803.01853 [hep-ph]].
- [3] L. Wang, J. M. Yang and Y. Zhang, “Two-Higgs-doublet models in light of current experiments: a brief review,” *Commun. Theor. Phys.* **74**, no.9, 097202 (2022); [arXiv:2203.07244 [hep-ph]].

- [4] N. S. Manton, “A New Six-Dimensional Approach to the Weinberg-Salam Model,” Nucl. Phys. B **158** (1979) 141-153.
- [5] D. B. Fairlie, “Higgs’ Fields And The Determination Of The Weinberg Angle,” Phys. Lett. B **82**, 97 (1979); “Two Consistent Calculations Of The Weinberg Angle,” J. Phys. G **5**, L55 (1979).
- [6] Y. Hosotani, “Dynamical Mass Generation by Compact Extra Dimension,” Phys. Lett. **126B** (1983) 309.
- [7] Y. Hosotani, “Dynamical of Non-integrable Phases and Gauge Symmetry Breaking,” ANNALS **190**, (1989) 233-253.
- [8] H. Hatanaka, T. Inami and C. S. Lim, “The Gauge hierarchy problem and higher dimensional gauge theories,” Mod. Phys. Lett. A **13**, 2601 (1998); [arXiv:hep-th/9805067].
- [9] I. Antoniadis, K. Benakli and M. Quiros, “Finite Higgs mass without supersymmetry,” New J. Phys. **3**, 20 (2001); [arXiv:hep-th/0108005].
- [10] N. Maru and T. Yamashita, “Two-loop calculation of Higgs mass in gauge-Higgs unification: 5D massless QED compactified on  $S^1$ ,” Nucl. Phys. B **754**, 127 (2006); [arXiv:hep-ph/0603237].
- [11] Y. Hosotani, N. Maru, K. Takenaga and T. Yamashita, “Two loop finiteness of Higgs mass and potential in the gauge-Higgs unification,” Prog. Theor. Phys. **118**, 1053 (2007); [arXiv:0709.2844 [hep-ph]].
- [12] C. S. Lim, N. Maru and K. Hasegawa, “Six dimensional gauge-Higgs unification with an extra space  $S^2$  and the hierarchy problem,” J. Phys. Soc. Jap. **77**, 074101 (2008); [arXiv:hep-th/0605180].
- [13] K. Hasegawa, C. S. Lim and N. Maru, “Predictions of the Higgs mass and the weak mixing angle in the 6D gauge-Higgs unification,” J. Phys. Soc. Jap. **85**, no.7, 074101 (2016); [arXiv:1509.04818 [hep-ph]].
- [14] C. A. Scrucca, M. Serone, L. Silvestrini and A. Wulzer, “Gauge Higgs unification in orbifold models,” JHEP **02**, 049 (2004); [arXiv:hep-th/0312267].

- [15] C. Csaki, C. Grojean and H. Murayama, “Standard model Higgs from higher dimensional gauge fields,” *Phys. Rev. D* **67**, 085012 (2003); [arXiv:hep-ph/0210133].
- [16] Y. Matsumoto and Y. Sakamura, “6D gauge-Higgs unification on  $T^2/Z_N$  with custodial symmetry,” *JHEP* **08**, 175 (2014); [arXiv:1407.0133 [hep-ph]].
- [17] Y. Hosotani, S. Noda and K. Takenaga, “Dynamical gauge-Higgs unification in the electroweak theory,” *Phys. Lett. B* **607**, 276-285 (2005); [arXiv:hep-ph/0410193].
- [18] K. Akamatsu, T. Hirose, N. Maru and A. Nago, “Electroweak Symmetry Breaking in Two Higgs Doublet Model from 6D Gauge-Higgs Unification on  $T^2/Z_2$ ,” [arXiv:2312.08608 [hep-ph]].
- [19] C. A. Scrucca, M. Serone and L. Silvestrini, “Electroweak symmetry breaking and fermion masses from extra dimensions,” *Nucl. Phys. B* **669**, 128-158 (2003); [arXiv:hep-ph/0304220 [hep-ph]].
- [20] G. Cacciapaglia, C. Csaki and S. C. Park, “Fully radiative electroweak symmetry breaking,” *JHEP* **0603**, 099 (2006); [arXiv:hep-ph/0510366].
- [21] M. Misiak and M. Steinhauser, “Weak radiative decays of the B meson and bounds on  $M_{H^\pm}$  in the Two-Higgs-Doublet Model,” *Eur. Phys. J. C* **77**, no.3, 201 (2017); [arXiv:1702.04571 [hep-ph]].
- [22] D. Fontes, M. Mühlleitner, J. C. Romão, R. Santos, J. P. Silva and J. Wittbrodt, “The C2HDM revisited,” *JHEP* **02**, 073 (2018); [arXiv:1711.09419 [hep-ph]].